Journal of Applied Polymer Science

Synthesis, Characterization, and Corrosion Inhibition Study of Polyaniline-α-Fe_2O_3 Nanocomposite

S. S. Umare, B. H. Shambharkar
Department of Chemistry, Visvesvaraya National Institute of Technology, Nagpur, Maharashtra 440 010, India
Correspondence to: S. S. Umare (E-mail: ssumare@chm.vnit.ac.in)

ABSTRACT: Polyaniline (PANI)-α-Fe_2O_3 nanocomposites (NCs) have been synthesized by chemical oxidative in situ polymerization of aniline in presence of α-Fe_2O_3 nanoparticles at 5°C using $(NH_4)_2S_2O_8$ as an oxidant in an aqueous solution of sodium dodecylbenzene sulphonic acid (SDBS), as surfactant and dopant under N_2 atmosphere. The room temperature conductivity of NCs decreases and coercive force (H_c) increases with an increase addition of α-Fe_2O_3 in PANI matrix. The result of FTIR and TGA shows that the interaction between α-Fe_2O_3 particles and PANI matrix could improve the thermal stability of NCs. NCs demonstrate the superparamagnetic behavior. The performance of PANI and PANI-α-Fe_2O_3 NCs as protective coating, against corrosion of 316LN stainless steel in 3.5% NaCl was assessed by potentiodynamic polarization technique. The study shows a good corrosion inhibition effect of both the coatings. © 2012 Wiley Periodicals, Inc. J. Appl. Polym. Sci. 000: 000–000, 2012

KEYWORDS: Conducting polymers; nanoparticles; nanocomposites; magnetic properties

Received 20 August 2011; accepted 24 March 2012; published online
DOI: 10.1002/app.37799

INTRODUCTION

Magnetic nanomaterials have been the subject of increasing interest because of their physical properties and technological applications.[1] The iron oxide (Fe_2O_3) has the important magnetic properties. From the viewpoint of the basic research, Fe_2O_3 oxide is a convenient compound for the general study of polymorphism and the magnetic and structural phase transitions of nanoparticles. The existence of amorphous Fe_2O_3 and its four polymorphs (α, β, γ, and ε) is well established. The most frequent polymorphs structure "α" (hematite) having a rhombohedral-hexagonal, prototype corundum structures, and cubic spinel structure "γ" (maghemite) have been found in nature. The other polymorphs, the cubic bixbyite structure "β" and orthorhombic structure "ε" and nanoparticles of all forms, have been synthesized and extensively investigated in recent years. γ- and ε-type Fe_2O_3 are ferromagnetic; α-Fe_2O_3 is a canted antiferromagnetic whereas β-type Fe_2O_3 is a paramagnetic material. In α-Fe_2O_3, the anions have a hexagonal close packed structure and the cations occupy 2/3 of the octahedral sites, i.e., oxygen occupies the hexagonal sites and the iron ions are situated only in the surrounding octahedral sites. α-Fe_2O_3 is paramagnetic above 956 K (T_c). At room temperature, it is weakly ferromagnetic and at 260 K (Morin temperature T_M), it undergoes a phase transition to an antiferromagnetic state.[2] Nanoparticles of α-Fe_2O_3 also exhibited this behavior, and T_M is found to be strongly dependent on the size of the particles.

α-Fe_2O_3 exhibit *n*-type semiconducting (E_g = 2.1 eV) properties[3] and is widely used in photoelectrodes, gas sensing, catalysts, magnetic recording, medical fields,[4] and electrode material[5] because of its low cost, high corrosion resistance,[6] and environmentally friendly properties. In addition, it is a vital photocatalyst in the degradation of 4-chlorophenol and the azo dye orange II under daylight irradiation,[7] methylene blue decomposition[8] and for photocatalytic hydrogen generation[9] and oxygen evolution.[10] Stimulated by the promising applications of the α-Fe_2O_3, various α-Fe_2O_3 nanostructures have been prepared by sol-gel,[11] high-energy ball milling,[12] hydrothermal method,[13] microwave-assisted hydrothermal method.[3] Among these methods, coprecipitation approach is an economical, simple, and promising way in the production of fine and uniform particles.[14–17]

Polyaniline (PANI) is a unique conducting polymer because of its chemical, environmental stability, its facile synthetic process, and its readily controlled doping level. PANI shows different properties with different dopants.[18–20] Organic dopant such as sodium dodecylbenzene sulphonic acid (SDBS) and CSA enhances the solubility whereas inorganic dopants such as HCl,

H_2SO_4, and HNO_3 enhance the electrical conductivity of PANI.[21] PANI-inorganic composites with electrical and magnetic properties[22] have potential applications in batteries, electrochemical display devices, electromagnetic interference shielding, electromagnetorheological fluids,[23] microwave-absorbing materials, and anticorrosion materials[24] because of their synergetic behaviors between conducting polymer and the inorganic magnetic nanoparticles. Several authors[21,25,26] have reported PANI and α-Fe_2O_3 as pigment in the coating. Sathiyanarayanan et al.[27] have reported PANI–α-Fe_2O_3 (commercially available, 2–3 μm) composites prepared by oxidative polymerization of aniline in phosphoric acid medium. The corrosion protection ability of the coating was found out by electrochemical impedance method in 3% NaCl solution. Nghia and Tung[24] have prepared PANI-Fe_2O_3.NiO nanocomposites (NCs) and investigated its protective performance in 3% NaCl solution by impedance measurement.

In our earlier communications,[28–30] we have reported PANI-Fe_3O_4, PANI-Co_3O_4, and PANI-NiO NCs with conducting and magnetic properties. Because NCs exhibit combination of properties like conductivity, electronic, electrochemical, catalytic, and optical properties. Therefore, herein an attempt has been made to generate novel NC intriguing electrical and magnetic properties by encapsulating the as synthesized α-Fe_2O_3 particles with PANI matrix. These properties may arise as a result of physical and chemical interactions between the inorganic oxide surface and the organic material.

In this article, α-Fe_2O_3 nanoparticles were synthesized by coprecipitation method. PANI-α-Fe_2O_3 NCs were synthesized by in situ polymerization of aniline in SDBS as surfactant and dopant, containing a dispersion of α-Fe_2O_3 nanoparticles (as prepared) where α-Fe_2O_3 is the magnetic and PANI is the conductive in nature. The influence of α-Fe_2O_3 content on the structural, thermal, electrical, magnetic, and anticorrosive properties of PANI-α-Fe_2O_3 NCs is reported.

EXPERIMENTAL

Materials

Aniline (Merck) was distilled before use and stored at 10°C. SDBS salt (25%), ammonium persulphate, anhydrous $FeCl_3$, urea $(NH_2)_2CO$, polyurethane clear (DuPont), 256 S Activator (DuPont), butanol, xylene, ethylene glycol, and double distilled water were used for preparing solutions.

Methods

Synthesis of α-Fe_2O_3 Nanoparticles. α-Fe_2O_3 nanoparticles were prepared by coprecipitation method.[15] One hundred milliliters $FeCl_3$ (0.2 *M*) solution, 10 g urea, and 200 mL ethylene glycol was taken in three-necked RB flask fitted with air condenser. The reaction mixture was mixed properly and then refluxed at 90°C for 2 h with continuous magnetic stirring. The dark brown precipitate was obtained. The precipitate was separated by centrifugation and washed with methanol and acetone. It was then dried at 100°C for 6 h in the air oven. Finally, the obtained product was calcined at 450°C for 2 h. Brown color α-Fe_2O_3 powder was obtained. Urea in the reaction gives homogenous precipitation because it gradually decomposes to produce carbonate ions and ammonia in aqueous solution at temperature about 80–100°C. On hydrolysis, reaction of iron chloride generates the precipitate of iron hydroxide and then on heat treatment gives rise to form α-Fe_2O_3 nanoparticles.

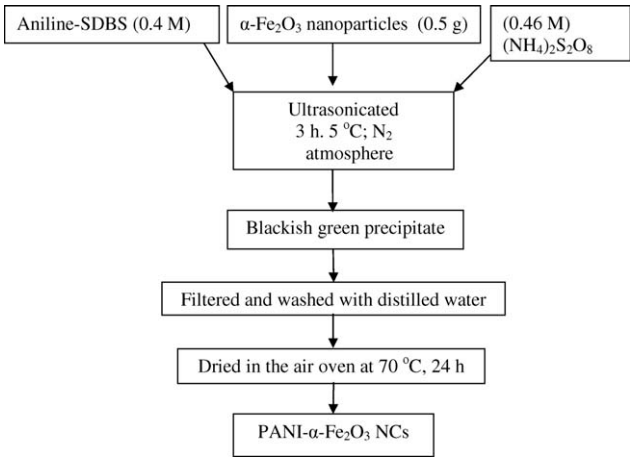

Scheme 1 . A schematic representation of synthesis of PANI-α-Fe_2O_3 NCs.

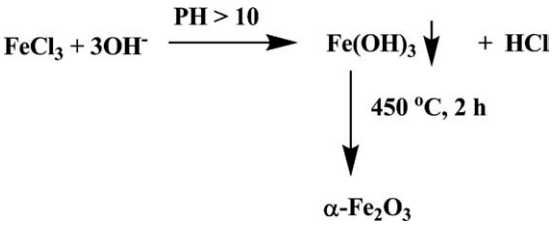

Synthesis of PANI-α-Fe_2O_3 NCs. The PANI-α-Fe_2O_3 (12.9 : 1) NC was prepared[28–30] by in situ chemical oxidative polymerization of aniline. One hundred milliliters solution containing 0.4 *M* aniline and 0.08 *M* SDBS, and 0.5 g of as synthesized α-Fe_2O_3 nanoparticles was taken in four-necked flat bottom flask. Then a precooled solution of ammonium persulphate (10.4972 g, 0.46 *M*) was added slowly to the reaction mixture containing aniline-SDBS solutions and α-Fe_2O_3 nanoparticles. The polymerization was allowed to proceed in N_2 atmosphere at 5°C for 3 h with continuous sonication. The molar ratio of aniline : SDBS and aniline : APS was 5 : 1 and 1 : 1.15, respectively. The reaction mixture was equilibrated for 4 h. The blackish green precipitate thus obtained was filtered, washed with distilled water until colorless filtrate was obtained and then dried in the air oven at 70°C for 24 h. Similarly, for comparison of properties composite of different molar ratios (6.5 : 1 and 4.3 : 1) of aniline to α-Fe_2O_3 was also been prepared. Scheme 1 shows a schematic representation of synthesis of PANI-α-Fe_2O_3 NCs.

Characterization

X-ray diffraction (XRD) analysis was conducted on X'Pert PRO, PANalytical X-ray diffractometer using CuKα radiation (λ = 1.5406 Å) at 45 kV and 40 mA. The measurements were performed in the 2θ range from 10 to 120°. Average crystallite size (t) of α-Fe_2O_3 particles was calculated from the line broadening using Scherrer's formula. $t = 0.9\lambda/\beta\text{Cos}\theta$, where, β is the full width at half maximum of the strongest peak, λ is the

X-ray wavelength (λ = 1.5406 Å), and θ is the angle of diffraction. Thermogravimetric analysis (TG/DTA) was performed on Pyris Diamond, Perkin–Elmer at the heating rate of 10°C/min in the temperature range from 30 to 1000°C under argon atmosphere with flow rate 200 mL/min.

Fourier transform infrared (FTIR) spectrums were recorded on Perkin–Elmer FTIR spectrophotometer (4000–450 cm^{-1}) with a 4.0 cm^{-1} resolution. KBr pellet technique was used to prepare sample for recording FTIR spectrum. Transmission electron microscopic (TEM) images were recorded on Philips, TEM CM 200 Supertwin.

Electrical conductivity of compressed pellets was measured at room temperature by two probe method. The pellets were prepared with the help of hydraulic press (Kimaya Engineers, India) by applying a pressure of 5000 kg/cm^2 for 30 s. D.C. resistance of pellets was measured on 928 auto LCR Q tester (Systronics). The conductivity value was calculated from the measured resistance and sample dimensions. Magnetization measurements were performed on Vibrating Sample Magnetometer (VSM) Model Oxford Maglab 14 Tesla VSM.

Corrosion inhibition study of PANI-α-Fe_2O_3 NCs was performed[31] by preparing formulation from 0.1 g of NC dispersed in 5 mL polyurethane binder, 2 mL hardener (256 S), and then mixture was stirred for 4 h. To modify the viscosity of the mixture, the xylene and butanol (4 : 1) was added in the formulated mixture. A drop (0.1 mL) of mixture was uniformly spread on the surface (1 cm^2) of 316LN stainless steel (SS) substrate and then it was dried at 60°C for 4 h. The thickness of coating was found to be 15–20 μm. Potentiodynamic polarization measurements were performed on Versa STAT 3 potentiostate. The experimental cell consist of three-electrode system with platinum gauge as counter electrode, saturated calomel electrode (SCE) as reference electrode and 316LN SS as working electrode. The potentiodynamic current–potential curves were recorded in the potential range from −500 to +500 mV (vs. SCE) at a scan rate of 2 mVs^{-1}. All the measurements were performed in aqueous 3.5% NaCl solution at room temperature (27°C).

RESULTS AND DISCUSSION

XRD Study

Figure 1(a-e) shows the typical XRD patterns of α-Fe_2O_3, PANI-α-Fe_2O_3 NCs, and PANI. The XRD pattern of the prepared α-Fe_2O_3 [Figure 1 (a)] reveals a Rhombohedral phase with cell parameters a = 5.03, c = 13.76 Å, (JCPDS file no. 80-2377), which is in good agreement with the values reported,[32] a = 5.03 Å, c = 13.74 Å (33-0664). The average crystallite size (t) of α-Fe_2O_3 particles was found to be 35 nm using Scherrer's relation. PANI-α-Fe_2O_3 composites [Figure 1(b–d)] shows all the sharp peaks of α-Fe_2O_3 and the broad peaks of PANI at 2θ = 20.41 and 25.61°, which is characteristic of PANI. The broad peaks of PANI becoming weaker on increasing the percentage of α-Fe_2O_3 in the composite.

FTIR Study

Figure 2(a–e) shows FTIR spectra of PANI, α-Fe_2O_3, and PANI-α-Fe_2O_3 NCs. Figure 2(e) show the characteristic absorption at 474 and 578 cm^{-1} correspond to the Fe—O vibrations in α-Fe_2O_3. PANI [Figure 2(a)] shows the peaks at 1504 and 1585 cm^{-1} correspond to the C=C stretching modes of benzenoid and quinoid ring. The peak at 826 cm^{-1} is assigned to out-of-plane C—H deformation of aromatic rings. The peak at 1154 cm^{-1} assigned to C—N stretching of secondary aromatic amine. The peak at 1307 cm^{-1} may be due to the presence of the C—$N^{\bullet+}$ stretching vibration in protonic acid doped PANI from SDBS-PANI, where SO_3 group of SDBS is bonded with N of PANI. The peak at 513 cm^{-1} is assigned to SO_3H of SDBS. FTIR spectrum of NCs [Figure 2(b–d)] shows all the prominent peaks of PANI[28–30] and Fe—O vibration of α-Fe_2O_3. However, C=N, C=C, and C—N absorption bands of PANI-α-Fe_2O_3 NCs were slightly shifted to lower wavenumbers when compared with that of PANI. This shift may be due to some electronic interaction between PANI chain and surface of α-Fe_2O_3. Scheme 2 shows the structure of SDBS-doped PANI-α-Fe_2O_3 NCs.

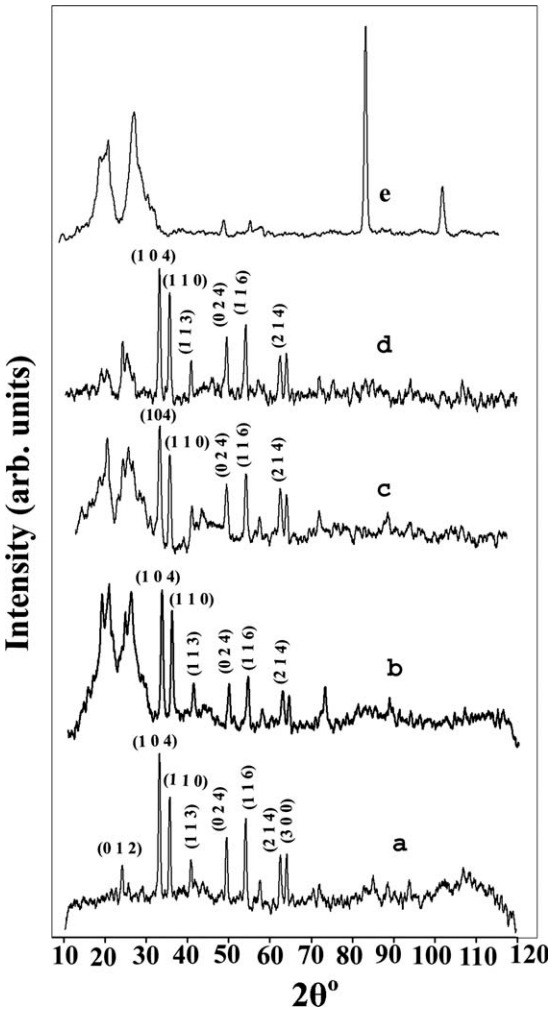

Figure 1. XRD patterns of (a) α-Fe_2O_3, (b) PANI-α-Fe_2O_3 (12.9 : 1) NC, (c) PANI-α-Fe_2O_3 (6.5 : 1) NC, (d) PANI-α-Fe_2O_3 (4.3 : 1) NC, and (e) PANI.

Morphological Studies

Figure 3(a–c) shows TEM images of the α-Fe_2O_3 and PANI-α-Fe_2O_3 NCs. α-Fe_2O_3 particles shows almost elliptical morphology. These particles are homodispersed. PANI-α-Fe_2O_3 NCs particles shows some aggregates may be because of their

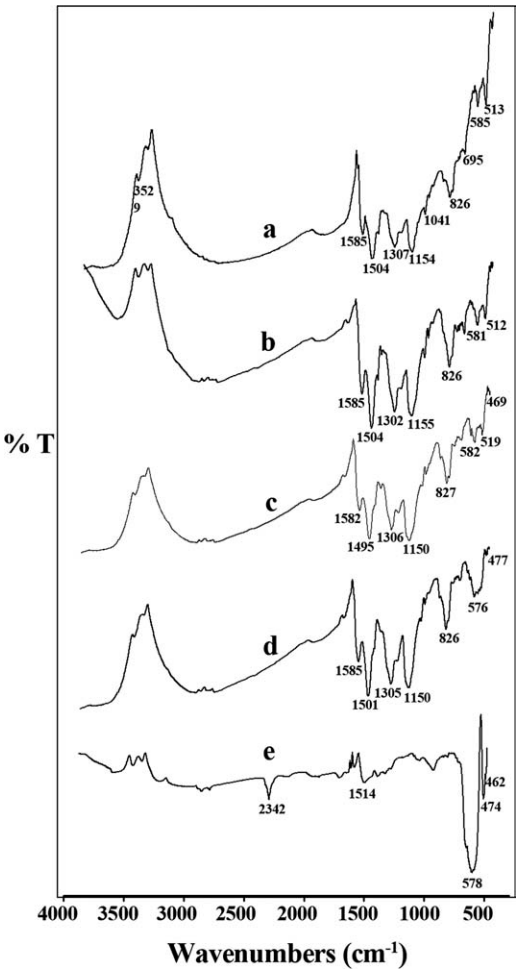

Figure 2. FTIR spectra of (a) PANI, (b) PANI-α-Fe_2O_3 (12.9 : 1), (c) PANI-α-Fe_2O_3 (6.5 : 1), (d) PANI-α-Fe_2O_3 (4.3 : 1) NCs, and (e) α-Fe_2O_3.

magnetodipole interparticle interactions. TEM image of NCs [Figure 3(b, c)] shows the existence of α-Fe_2O_3 nanoparticles in PANI matrix. The size of α-Fe_2O_3 particles obtained in composite is found to be similar as that obtained from the XRD study.

Thermal Study

TG thermogram of α-Fe_2O_3, PANI, and PANI-α-Fe_2O_3 NCs are shown in Figure 4(a–e). PANI shows three steps weight loss. The initial weight loss up to ~ 105°C is due to residual water, and loss above 200°C may be due to loss of SDBS and thermal degradation of PANI started after 300°C. PANI-α-Fe_2O_3 NCs shows similar decomposition steps of PANI but it has high stability. To compare the relative thermal stability of α-Fe_2O_3, PANI, and PANI-α-Fe_2O_3, % weight loss at different temperatures are reported (Table I). The thermal stability of PANI-α-Fe_2O_3 is more compared with PANI. The improvement in the thermal stability of NCs may be due to some interaction of PANI and α-Fe_2O_3. On increasing the content of α-Fe_2O_3 in NCs, the thermal stability of NCs is increasing due to more incorporation of inorganic component in the composite.

Electrical and Magnetic Properties

PANI shows the room temperature electrical conductivity as 3.26×10^{-4} S/cm. However, PANI-α-Fe_2O_3 NCs conductivity is less (Table II). Such decrease in conductivity is due to the presence of semiconducting α-Fe_2O_3 nanoparticles which partially baffle the formation of conductive paths that may decrease the doping level in the NCs. The PANI-α-Fe_2O_3 NCs conductivity did not show significant change on variation of α-Fe_2O_3 in NCs, which may be due to semiconducting nature of α-Fe_2O_3.

Figure 5(a–e) shows M–H curves of PANI, α-Fe_2O_3, and PANI-α-Fe_2O_3 NCs. Under an applied magnetic field 3 T, both the constituents and NCs shows the positive magnetization. At 5 K, α-Fe_2O_3 nanoparticles has remanent magnetization (M_r) = 3.68 × 10^{-3} emu/g and coercivity (H_c) = 2.74 × 10^{-1} T (Table II) and exhibit ferromagnetic behavior, whereas PANI is

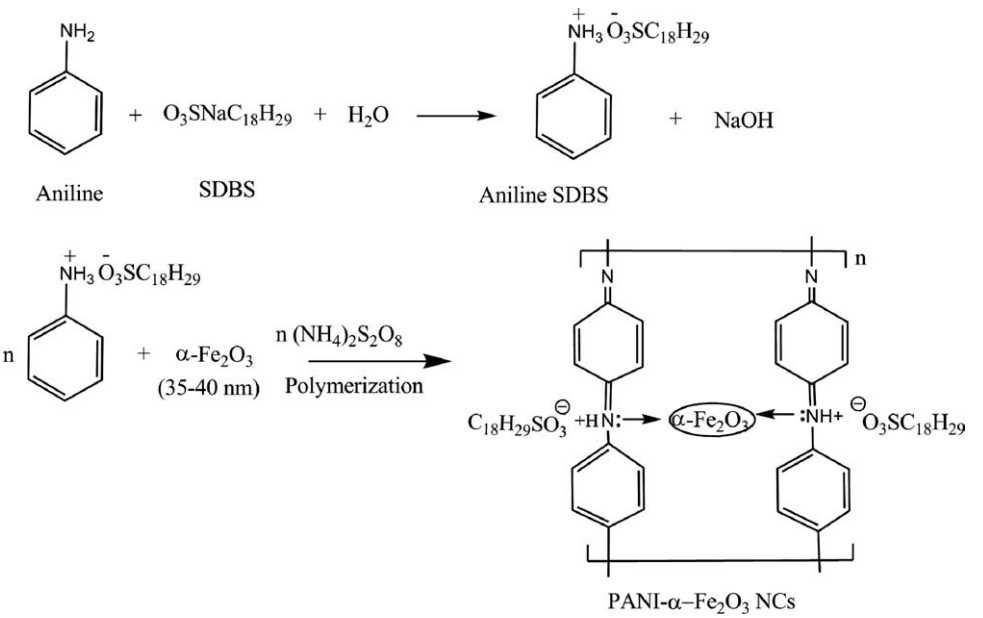

Scheme 2. Structure of PANI-α-Fe_2O_3 NCs.

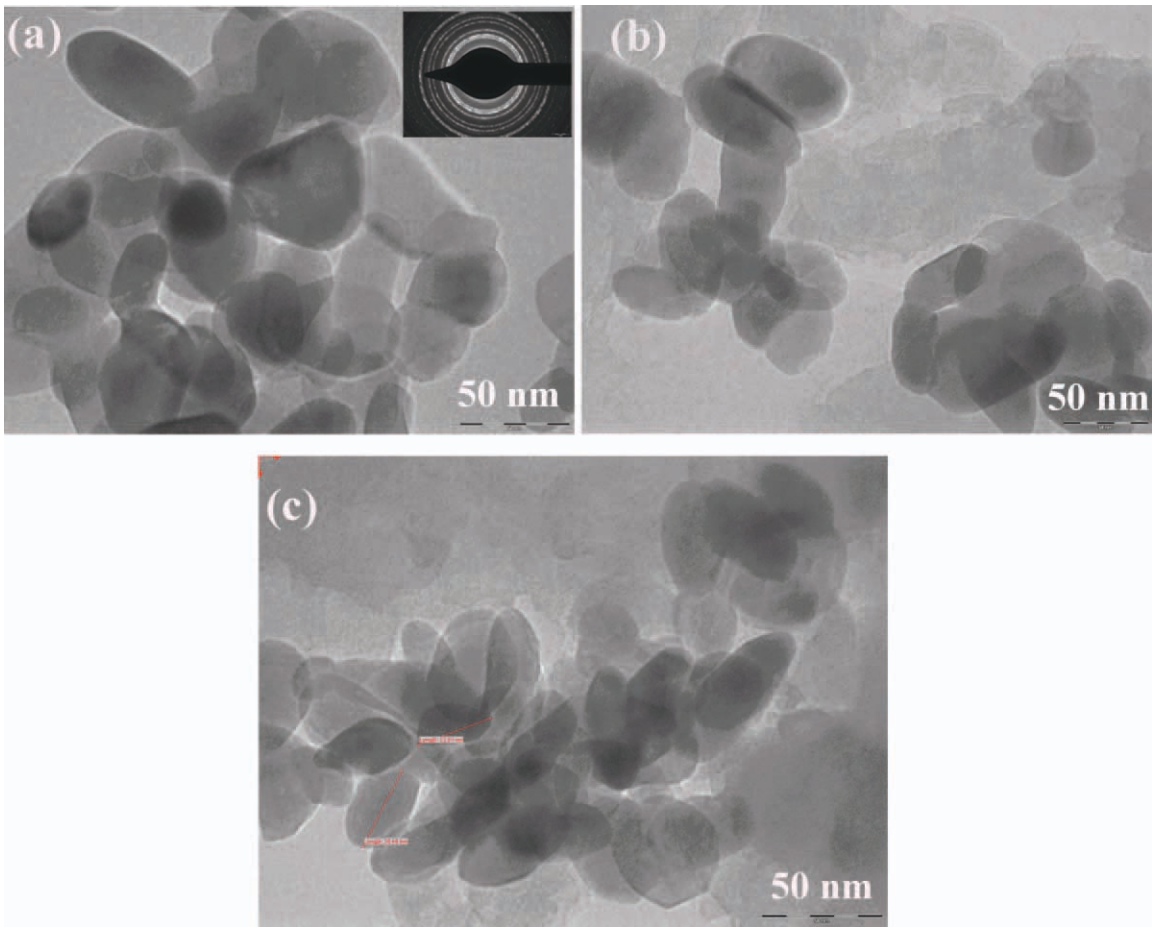

Figure 3. TEM images of (a) α-Fe_2O_3, (b) PANI-α-Fe_2O_3 (12.9 : 1), and (c) PANI-α-Fe_2O_3 (4.3 : 1) NCs. [Color figure can be viewed in the online issue, which is available at wileyonlinelibrary.com.]

paramagnetic. At lower temperatures, the spins are freezing. The system suffers from the Peierls instability, and thus the electrons are localized giving rise to a metal-semiconducting transition and an associated paramagnetism.[33] On incorporating α-Fe_2O_3 nanoparticles into PANI matrix, a typical 'S'-like shape of hysteresis was appeared in NCs, indicating their superparamagnetic[34] property. In addition, the H_c value is found to be increased with the increase of α-Fe_2O_3 content in composite. This indicates the magnetic property of composite dependence on α-Fe_2O_3 content in it.

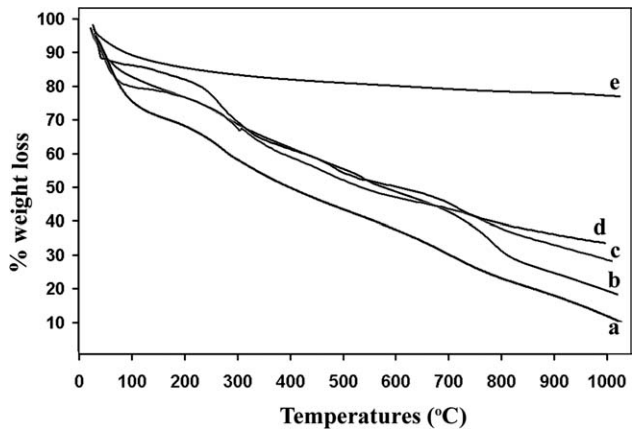

Figure 4. TG thermogram of (a) PANI, (b) PANI-α-Fe_2O_3 (12.9 : 1), (c) PANI-α-Fe_2O_3 (6.5 : 1), (d) PANI-α-Fe_2O_3 (4.3 : 1) NCs, and (e) α-Fe_2O_3.

Corrosion Inhibition Study

Figure 6(a–d) shows the potentiodynamic tafle plots of bare 316LN SS, and 316LN SS coated with PANI and NCs. The values of corrosion potential (E_{corr}) and corrosion current density (I_{corr}) are given in Table II. On comparison of I_{corr} of bare sample with that of PANI and NCs-coated SS samples, it is observed that, I_{corr} of PANI-coated sample is 100 times less and

Table 1. % Weight Loss Data for PANI, α-Fe_2O_3, and PANI-Fe_2O_3 NCs at Different Temperatures

Samples	% Weight loss			
	110°C	300°C	500°C	700°C
PANI	25.37	44.66	71.42	77.55
Fe_2O_3	07.48	12.58	14.84	17.53
PANI-Fe_2O_3 (12.9 : 1)	15.0	28.83	42.71	56.20
PANI-Fe_2O_3 (6.5 : 1)	11.24	22.53	45.89	70.53
PANI-Fe_2O_3 (4.3 : 1)	11.73	24.43	40.02	57.15

Table II. Room Temperature Conductivity and Magnetic Parameters of PANI, α-Fe_2O_3, and PANI-α-Fe_2O_3 NCs measured at 5 K; Potentiodyanamic Parameters of Bare, PANI, and PANI-α-Fe_2O_3 NCs-Coated Samples

Samples	Conductivity (S/cm)	M_r (emu/g)	H_c (T)	I_{corr} (μA/cm^2)	E_{corr} (mV)
α-Fe_2O_3	–	3.68×10^{-3}	2.74×10^{-1}	–	–
PANI	3.26×10^{-4}	6.02×10^{-5}	6.51×10^{-2}	0.0367	-207
PANI-α-Fe_2O_3 (12.9 : 1)	6.1×10^{-5}	5.51×10^{-4}	2.64×10^{-2}	0.00033	-251.55
PANI-α-Fe_2O_3 (6.5 : 1)	5.54×10^{-5}	4.39×10^{-4}	2.77×10^{-2}	0.00011	-246.86
PANI-α-Fe_2O_3 (4.3 : 1)	6.0×10^{-5}	1.73×10^{-3}	2.73×10^{-2}	–	–
Bare	–	–	–	13.11	-522

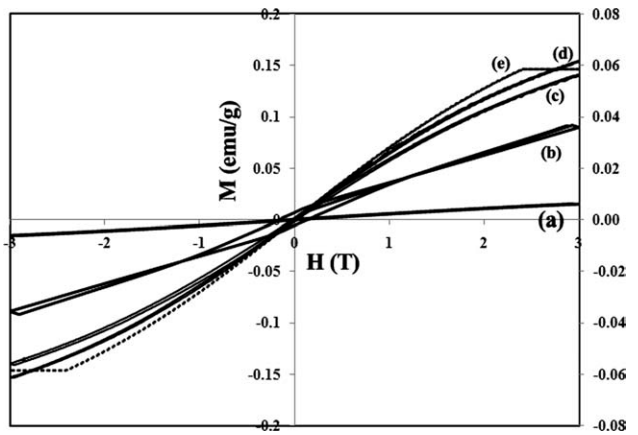

Figure 5. Magnetization versus applied field data of (a) PANI, (b) α-Fe_2O_3, (c) PANI-α-Fe_2O_3 (12.9 : 1), (d) PANI-α-Fe_2O_3 (6.5 : 1), and (e) PANI-α-Fe_2O_3 (4.3 : 1) NCs measured at 5 K.

that for NC-coated sample is 10^4 times less than the bare sample. This lower value of I_{corr} of coated sample may be due to the formation of a protective layer. It is suggested[35] that corrosion protection occurs via formation of passivating layer and conducting polymer acts as an electronic and chemical diffusion barrier in preventing corrosion rather than merely playing the role as a physical barrier. NCs show the synergetic effects to prevent corrosion. Because α-Fe_2O_3 is n-type and PANI behaves as a p-type semiconductor, it is quite likely that both these species may form p-n junctions, which prevent easy charge transport across the layer. The synergetic action between α-Fe_2O_3, PANI-SDBS hinder the process of electron or charge to transfer across the film. Thus, the barrier property of the coating gets enhanced significantly and as a consequence flow of electrons or ions in and through the film is hindered. Similar type of results[35,36] was also been reported earlier.

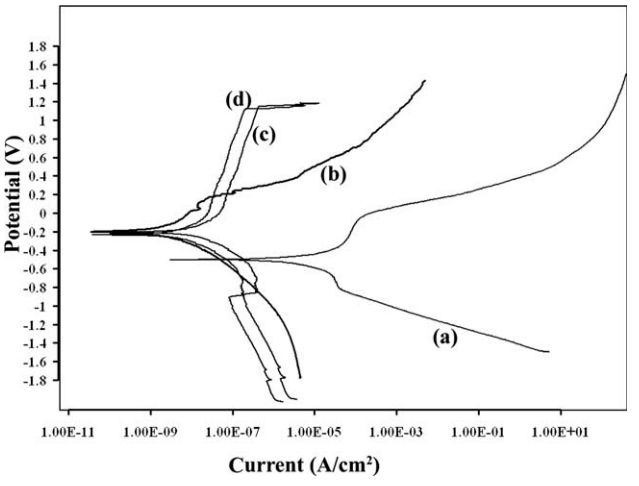

Figure 6. Tafle plots of (a) bare 316LN SS (b) PANI, (c) PANI-α-Fe_2O_3 (12.9 : 1), and (d) PANI-α-Fe_2O_3 (6.5 : 1) NCs coated on 316LN.

CONCLUSIONS

PANI-α-Fe_2O_3 NCs have been prepared by in situ chemical oxidative polymerization of aniline. The results of XRD, FTIR, TGA, and TEM reveal the formation of NCs. The conductivity of PANI-α-Fe_2O_3 NCs decreases after addition of α-Fe_2O_3 because of the blocking of PANI conductive pathways by α-Fe_2O_3. The magnetization results showed that the prepared α-Fe_2O_3 nanoparticles and PANI exhibit ferromagnetic and paramagnetic character, respectively, whereas NCs demonstrate superparamagnetic behavior. Potentiodynamic study demonstrates that the PANI and NCs has excellent corrosion protection properties in aqueous 3.5% NaCl solution by formation of p-n junction, which restricts the charge transport across the layer.

ACKNOWLEDGMENTS

The authors thank Department of Condensed Matter Physics and Material Science, TIFR Mumbai for VSM measurements. One of the authors B. H. Shambharkar is thankful to Director, Visvesvaraya National Institute of Technology Nagpur for awarding research fellowship.

REFERENCES

1. Cao, M.; Liu, T.; Gao, S.; Sun, G.; Wu, X.; Hu, C.; Wang, Z. L. *Angew. Chem. Int. Ed.* **2005,** *44*, 2.
2. Bhowmik, R. N.; Saravanan, A. *J. Appl. Phys.* **2010,** *107*, 053196.
3. Zhang, X.; Li, Q. *Mater. Lett.* **2008,** *62*, 988.
4. Lee, Yu.-C.; Chueh, Y.-L.; Hsieh, C.-H.; Chang, M.-T.; Chou, L.-J.; Wang, Z. L.; Lan, Y.-W.; Chen, C.-D.; Kurata, H.; Isoda, S. *Small* **2007,** *3*, 1356.
5. Reddy, M. V.; Yu, T.; Sow, C.-H.; Shen, Z. X.; Lim, C. T.; Subba Rao, G. V.; Chowdari, B.V. R. *Adv. Funct. Mater.* **2007,** *17*, 2792.

6. Zeng, S.; Tang, S. K.; Li, T. *J. Colloid Interface Sci.* **2007,** *312*, 513.
7. Bandara, J.; Klehm, U.; Kiwi, *J. Appl. Catal. B* **2007,** *76*, 73.
8. Qurashi, A.; Zhong, Z.; Alam, M. W. *Solid State Sci.* **2010,** *12*, 1516.
9. Boudjemaa, A.; Boumaza, S.; Trari, M.; Bouarab, R.; Bouguelia, A. *Int. J. Hydrogen Energy* **2009,** *34*, 4268.
10. Boumaza, S.; Boudjemaa, A.; Omeiri, S.; Bouarab, R.; Bouguelia, A.; Trari, M. *Sol. Energy* **2010,** *84*, 715.
11. Woo, K.; Lee, H. J.; Ahn, J.-P.; Park, Y. S. *Adv. Mater.* **2003,** *15*, 1761.
12. Wang, L.-L.; Jiang, J.-S. *Phys. B* **2007,** *390*, 23.
13. Giri, S.; Samanta, S.; Maji, S.; Ganguli, S.; Bhaumik, A. *J. Magn. Magn. Mater.* **2005,** *285*, 296.
14. Prasad, S. Dissertation, Indian Institute of Technology Kanpur, India, **1997.**
15. Umare, S. S.; Ninghthuojam, R. S.; Sharma, S. J.; Shrivastava, S.; Kurian, S.; Gajbhiye, N. S. *Hyperfine Interact.* **2008,** *184*, 235.
16. Klabunde, K. J.Ed. Nanoscale Materials in Chemistry; Chapter 4, Wiley: NewYork, **2001.**
17. Ninghthuojam, R. S.; Gajbhiye, N. S., Ahmad, A.; Umare, S. S.; Sharma, S. J. *J. Nanosci. Nanotech.* **2008,** *8*, 3059.
18. Gupta, M. C.; Umare, S. S. *Macromolecules* **1992,** *25*, 138.
19. Inoue, M.; Navarro, R. E.; Inoue, M. B. *Synth. Met.* **1989,** *30*, 199.
20. Cao, Y.; Smith, P.; Heeger, A. *Synth. Met.* **1992,** *48*, 91.
21. Rathod, R. C.; Didolkar, V. K.; Umare, S. S.; Shambharkar, B. H. *Trans. Indian Inst. Met.* **2011,** *64*, 431.
22. Qiu, G.; Wang, Q.; Nie, M. *J. Appl. Polym. Sci.* **2006,** *102*, 2107.
23. Fang, F. F.; Kim, J. H.; Choi, H. J.; Seo, Y. *J. Appl. Polym. Sci.* **2007,** *105*, 1853.
24. Nghia, N. D.; Tung, N. T. *Synth. Met.* **2009,** *159*, 831.
25. MacDiarmid, A. G.; Chiang, J. C.; Richter, A. F. *Synth. Met.* **1987,** *18*, 285.
26. Zarras, P.; Anderson, N.; Webber, C.; Irvin, D. J.; Irvin, J. A.; Guenthner, A. Stenger-Smith, J. D. *Radiat. Phys. Chem.* **2003,** *68*, 387.
27. Sathiyanarayanan, S.; Syed Azim, S.; Venkatachari, G. *Synth. Met.* **2007,** *157*, 751.
28. Umare, S. S.; Shambharkar, B. H.; Ninghthuojam, R. S. *Synth. Met.* **2010,** *160*, 1815.
29. Shambharkar, B. H.; Umare, S. S. *Mater. Sci. Eng. B* **2010,** *175*, 120.
30. Shambharkar, B. H.; Umare, S. S. *J. Appl. Polym. Sci.* **2011,** *122*, 1905.
31. Kalendová, A.; Veselý, D.; Stejskal, *J. Prog. Org. Coat.* **2008,** *62*, 105.
32. Mitra, S.; Das, S.; Basu, S.; Sahu, P.; Mandal, K. *J. Magn. Magn. Mater.* **2009,** *321*, 2925.
33. Dallas, P.; Stamopoulos, D.; Boukos, N.; Tzitzios, V.; Niarchos, D.; Petridis, D. *Polymer* **2007,** *48*, 3162.
34. Kumar, S.; Singh, V.; Aggarwal, S.; Mandal, U. K.; Kotnala, R. K. *Compos. Sci. Technol.* **2010,** *70*, 249.
35. Radhakrishnan, S.; Siju, C. R.; Mahanta, D.; Patil, S.; Madras, G. *Electrochim. Acta* **2009,** *54*, 1249.
36. Patil, R. C.; Radhakrishnan, S. *Prog. Org. Coat.* **2006,** *57*, 332.